Three-Dimensional Networks

A Three-Dimensional Ferrimagnet Composed of Mixed-Valence Mn_4 Clusters Linked by an $\{Mn[N(CN)_2]_6\}^{4-}$ Unit**

Hitoshi Miyasaka, Kazuya Nakata, Ken-ichi Sugiura, Masahiro Yamashita, and Rodolphe Clérac**

In the field of molecule-based magnetism, tremendous effort has been devoted to the design of magnetic materials that exhibit spontaneous magnetization.[1] The molecular approach offers a unique opportunity to choose beforehand the properties of precursors and magnetic bridges to obtain magnets with desired physical properties. This strategy has already led to fascinating compounds that exhibit multifunctional physical properties.[2–4] Among the available building blocks, single-molecule magnets (SMMs) are one of the most appealing. SMMs have a large spin ground state together with a strong uniaxial anisotropy, which leads to a slow relaxation of their magnetization.[5] Therefore, these clusters can be seen as monodisperse superparamagnetic particles capable of storing information at the molecular level. Recently, Wernsdorfer et al. reported a new material composed of antiferromagnetically coupled dimeric units of SMMs.[6] They discovered that the presence of weak magnetic interactions between SMMs allows a fine tuning of the quantum properties. Their conclusions open new perspectives on the design of new magnetic materials by using SMM clusters as the building block to create more complicated architectures. In this vein, a 3D network of magnetically coupled SMMs could lead to new magnetic behavior induced by the intrinsic properties carried by these magnetic units (such as high spin state, Ising type anisotropy, quantum effects). Herein, we present the first example of such 3D magnetic materials, $[Mn_4(hmp)_4(OH)_2Mn(dcn)_6]\cdot 2\,MeCN\cdot 2\,THF$ (**1**) (Hhmp = hydroxymethylpyridine, Hdcn = dicyanamine), built on a well-known Mn_4 SMM, reported by Hendrickson, Christou,

[*] Dr. H. Miyasaka, K. Nakata, Prof. K.-i. Sugiura, Prof. M. Yamashita[+]
Department of Chemistry, Graduate School of Science
Tokyo Metropolitan University
1-1 Minami-Ohsawa, Hachioji, Tokyo 192-0397 (Japan)
and "Structural Ordering and Physical Properties"
PRESTO, Japanese science and technology agency
4-1-8 Honcho Kawaguchi, Saitama 332-0012 (Japan)
Fax: (+81) 426-77-2525
E-mail: miyasaka@comp.metro-u.ac.jp
Dr. R. Clérac
Centre de Recherche Paul Pascal, CNRS UPR 8641
115 avenue du Dr. A. Schweitzer, 33600 Pessac (France)
Fax: (+33) 5-56-84-56-00
E-mail: clerac@crpp-bordeaux.cnrs.fr
[+] CREST, Japanese science and technology agency
4-1-8 Honcho Kawaguchi, Saitama 332-0012 (Japan)

[**] This work was supported by PRESTO (H.M.) and CREST (M.Y.), Japanese science and technology agencies. R.C. would like to thank the CNRS, the Université de Bordeaux I and the Conseil Regional d'Aquitaine for financial support. We thank Prof. Claude Coulon for fruitful discussions.

 DOI: 10.1002/ange.200353093

and co-workers,[7] linked by dicyanamide $N(CN)_2^-$ to paramagnetic Mn^{II} centres.

Compound **1** has been obtained by a self-assembly reaction in a basic MeCN/THF solution that contained $[Mn(H_2O)_2](ClO_4)_x$, hmp^- ions, and $NaN(CN)_2$ in a molar ration of 1:2:1, respectively. The resulting solution was then filtered and single crystals suitable for X-ray diffraction were obtained by slow diffusion of THF. The crystal-structure analysis of **1** revealed a covalently bonded 3D structure that crystallizes in monoclinic space group, $P2_1/n$ ($Z=2$). The 3D network is composed of two basic units: a mixed-valence $Mn_4^{II,III}$ cationic complex, $\{Mn_4(hmp)_4(\mu_3\text{-}OH)_2\}^{4+}$, and an octahedral Mn^{II} anionic moiety, $\{Mn[N(CN)_2]_6\}^{4-}$, in a 1:1 ratio (Figure 1). The Mn_4 cluster unit has a rhombic core quasi-identical to one observed for $[Mn_4(hmp)_6Br_2(H_2O)_2]Br_2\cdot 4H_2O$.[7] The four Mn ions are hexacoordinated and arranged in a double-cuboidal fashion. Two different sites of Mn ions can be identified. The Mn(2) sites (Mn(2) and Mn(2*)) are individually chelated by two hmp^- ligands, which are *cis* to each other, and are interconnected by two hydroxy O(1) bridges to form a $\{(hmp)_2Mn(2)\text{–}(OH)_2\text{–}Mn(2^*)(hmp)_2\}$ motif lying on an inversion center (* symmetry operation: $-x$, $-y$, $-z$). This moiety is connected to the two Mn(1) centers (Mn(1) and Mn(1*)) by the hydroxy oxygen atom (μ_3-O(1)), and alkoxy oxygen atoms arising from the hmp^- ligands (μ_2-O(2) and O(3)), thus forming the Mn_4 cluster core, $\{Mn_4(hmp)_4(\mu_3\text{-}OH)_2\}^{4+}$ (Figure 1). The octahedral coordination sphere of Mn(1) ion is completed by three nitrogen atoms of $N(CN)_2^-$ ligands. The other side of each $N(CN)_2^-$ is connected to a monomeric Mn^{II} ion, Mn(3). Six $N(CN)_2^-$ bridging ligands make the coordination sphere of Mn(3) octahedron and finally form a $\{Mn[N(CN)_2]_6\}^{4-}$ unit. Each of these $\{Mn_4(hmp)_4(\mu_3\text{-}OH)_2\}^{4+}$ and $\{Mn[N(CN)_2]_6\}^{4-}$ units is linked to six different neighbors with opposite charge to form the 3D network of **1** shown in Figure 2. The oxidation states of the three Mn ion sites, Mn(1) and Mn(2) ions in the cluster moiety and Mn(3) ion of $\{Mn[N(CN)_2]_6\}^{4-}$ unit, can be easily assigned as divalent, trivalent, and divalent, respectively, based on charge balance consideration, bond valence sum calculation,[8] and the presence on Mn(2) of Jahn–Teller elongation axis (N(2)–Mn(2)–O(1*); Figure 1). As expected for typical Mn^{II} ions, bond lengths around Mn(1) and Mn(3) are found in the range of 2.174(4) to 2.278(5) Å. On the other hand, bond lengths around the Mn(2) are significantly longer in the axial position (N(2)-Mn(2) = 2.213(5) Å and O(1*)-Mn(2) = 2.220(3) Å) than in the equatorial plane (average value of 1.961 Å), thus revealing a Jahn–Teller distortion. On a particular Mn_4 cluster, Jahn–Teller axes on Mn(2) and Mn(2*) are parallel to each other and individually slightly bent N(2)-Mn(2)-O(1*) = 159.6(1)°.

The temperature dependence of the magnetic susceptibility was measured on a nujol-restrained polycrystalline

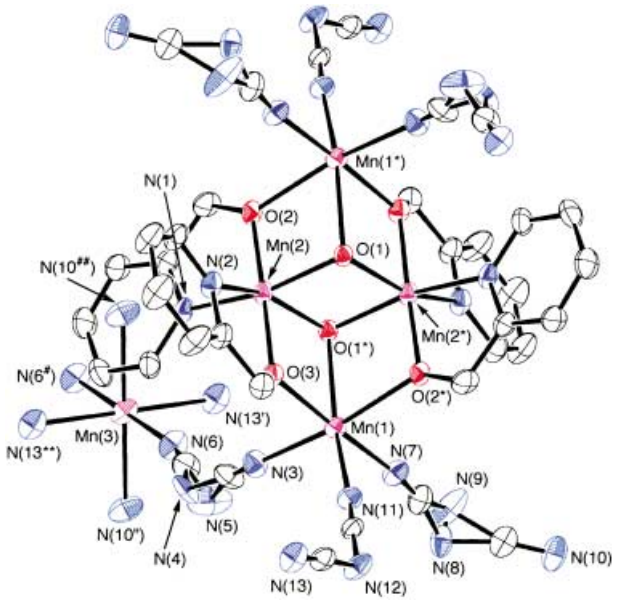

Figure 1. Structure of the repeating unit in **1** with thermal ellipsoids set at 30% probability. Hydrogen atoms and crystallization solvents are omitted for clarity.

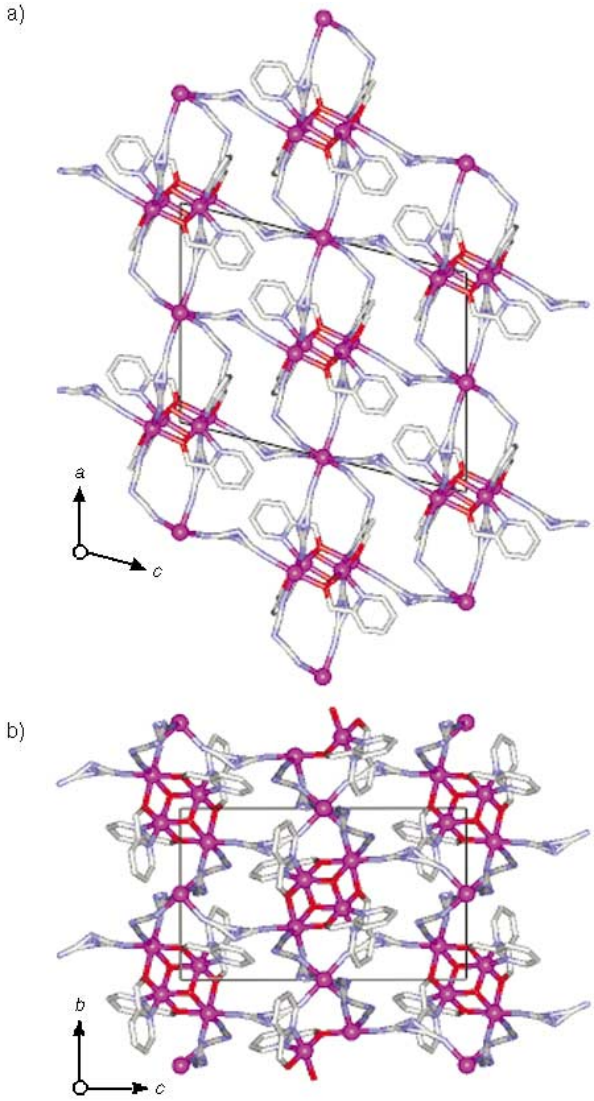

Figure 2. Perspective views of 3D packing of **1** in the *ac* (a) and *bc* (b) planes; C gray; N blue; O red; Mn purple.

sample of **1** in the temperature range of 1.8 K to 300 K under 1 kOe.[9] Above 100 K, the $1/\chi$ product (χ is the magnetic suscepitibility) obeys the Curie-Weiss law with $C = 18.15\ cm^3\,K\,mol^{-1}$ and $\theta = +20.2$ K; C is the Curie constant, θ is the Weiss constant.[10] Based on the interaction mediated by dicyanamide being relatively small,[11] the positive Weiss constant indicates that ferromagnetic exchange interactions are dominant in the Mn_4 unit. With lowering temperature, the χT product (19.38 $cm^3\,K\,mol^{-1}$ at 300 K) increases gradually in the temperature range of 300 to 30 K and then abruptly to reach a maximum of 186.2 $cm^3\,K\,mol^{-1}$ at 3.7 K (Figure 3). At

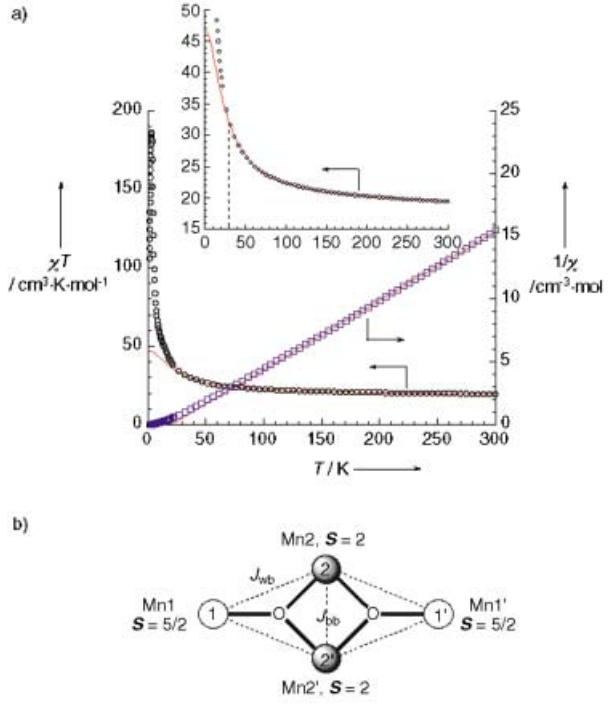

Figure 3. a) Temperature dependence of the χT product and $1/\chi$ measured on a Nujol-restrained polycrystalline sample of **1** under 1 kOe. The solid line represents a best-fitting simulation using a Kambe model to describe the Mn_4 unit susceptibility (see text). b) Schematic representation of the exchange coupling in the Mn_4 core of **1** with principal exchange pathways J_{wb} and J_{bb}.

lower temperatures, the χT decreases to 105.6 $cm^3\,K\,mol^{-1}$ at 1.8 K. It should be noted here that if a Curie contribution ($S = 5/2$, $g = 2$; S is the spin angular momentum, g is the g factor) of the $\{Mn[N(CN)_2]_6\}^{4-}$ unit is removed, the magnetic behavior of **1** above 50 K can be almost overlapped to the one observed for $[Mn_4(hmp)_6Br_2(H_2O)_2]Br_2{\cdot}4\,H_2O$.[7] Therefore, a similar analysis of the magnetic data has been performed by using the Kambe vector-coupling method.[12] Based on the structure analysis, the number of magnetic interactions can be reduced significantly: $J_{1'2} = J_{1'2'} = J_{12} = J_{12'} = J_{wb}$, $J_{22'} = J_{bb}$ (see Figure 3b; J = magnetic exchange interactions), hence the Hamiltonian can be written: [Eq (1)]

$$\mathscr{H} = \{-J_{wb}(\boldsymbol{S}_T^2 - \boldsymbol{S}_A^2 - \boldsymbol{S}_B^2) - J_{bb}(\boldsymbol{S}_A^2 - \boldsymbol{S}_1^2 - \boldsymbol{S}_{1'}^2) + g_{av}\,\mu_B\,\boldsymbol{S}_T\,\boldsymbol{H}\} + g_{Mn^{II}}\,\mu_B\,\boldsymbol{S}_{Mn^{II}}\,\boldsymbol{H} \quad (1)$$

in which $\boldsymbol{S}_A = \boldsymbol{S}_1 + \boldsymbol{S}_{1'}$, $\boldsymbol{S}_B = \boldsymbol{S}_2 + \boldsymbol{S}_{2'}$, $\boldsymbol{S}_T = \boldsymbol{S}_A + \boldsymbol{S}_B$ (the spin operators $\boldsymbol{S}$ are given in Figure 3b) g_{av} is the average g value of the Mn_4 unit. In Equation (1), the first term is modeling the magnetic behavior of the Mn_4 core and the latter is related to the Mn^{II} paramagnetic center of $\{Mn[N(CN)_2]_6\}^{4-}$ unit. Fitting of the experimental data between 30 and 300 K leads to $g_{av} = 1.95$, $g_{Mn^{II}} = 2.00$, $J_{wb}/k_B = +1.5$ K, $J_{bb}/k_B = +7.1$ K, $TIP = 600 \times 10^{-6}\ cm^3\,mol^{-1}$ (fixed; TIP = temperature-independent paramagnetism, and k_B is the Boltzmann constant). The estimated values of intracluster magnetic exchange interactions, J_{wb} and J_{bb} are similar to the values reported for $[Mn_4(hmp)_6Br_2(H_2O)_2]Br_2{\cdot}4\,H_2O$, and associated with an $S = 9$ spin ground state for the Mn_4 unit in **1**. Below 30 K, the magnetic interaction (J_{3D}) mediated by dicyanamide bridges between $\{Mn_4(hmp)_4(\mu_3\text{-}OH)_2\}^{4+}$ and $\{Mn[N(CN)_2]_6\}^{4-}$ units becomes relevant and the previous model cannot reproduce the experimental data.

As shown in Figure 4, in-phase ac magnetic susceptibility, χ', exhibits a peak located around 4 K and out-of-phase ac susceptibility, χ'', leaves from zero at 4.1 K. This behavior was found to be independent on the ac frequency used, which indicates the presence of a 3D magnetic ordering at about 4.1 K.

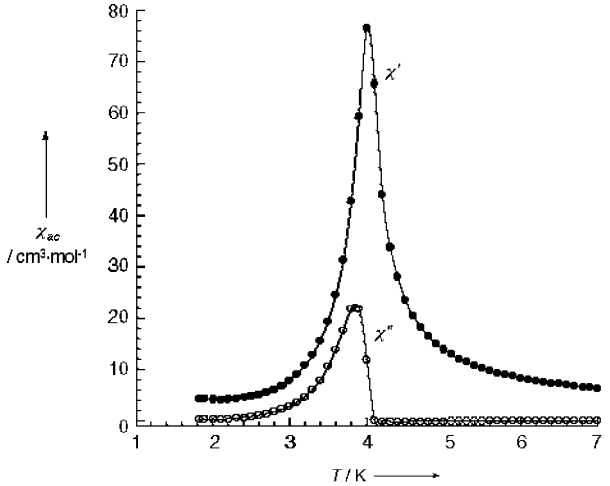

Figure 4. Temperature dependence of ac susceptibilities, in-phase (χ') and out-of-phase (χ'') measured on a Nujol-restrained polycrystalline sample of **1** at 1200 Hz (in zero applied dc field and 3 Oe oscillating ac field).

A hysteresis loop of the magnetization is observed as a function of external field at 1.9 K with a small coercive field of 28 Oe (Figure 5a). This feature disappears when the temperature reaches about 4.1 K, which indicates a long-range magnetic transition at this temperature. The magnetization was also measured up to 7 T (Figure 5b, at 1.9 K). At low fields, as expected for a magnet, the magnetization abruptly rises up to around 11 μ_B at 2 kOe. This magnetization is close to the expected value of 13 μ_B ($g = 2$) for an ordered ferrimagnetic phase in which the $S = 9$ Mn_4 units are antiferromagnetically coupled with the $S = 5/2$

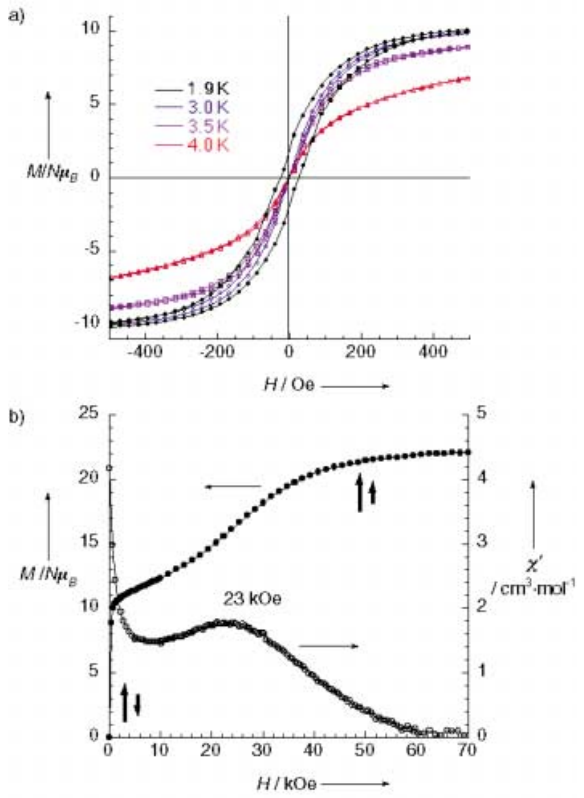

Figure 5. a) Field dependence of magnetization (hysteresis loops) measured on a Nujol-restrained polycrystalline sample of **1** below 4.0 K in the field of ±500 Oe and b) field dependence of magnetization and the in-phase ac susceptibility at 1.9 K (ac frequency, 10 Hz; oscillating ac field, 3 Oe and zero applied dc field).

$\{Mn[N(CN)_2]_6\}^{4-}$ units. When the field is further increased, the magnetization gradually reaches 22 μ_B (at 7 T), value close to the one expected for all parallel oriented spins (23 μ_B with $g=2$). This field-induced behavior is expected for ferrimagnetic systems[13,14] when the strength of the magnetic interaction between spin carriers is overcome by an applied magnetic field (H_c). The sigmoidal shape of the magnetization or the maximum observed on the χ' versus H plot is a characteristic feature associated with a spin flipping of one of the two ferrimagnetic sublattices. Because of the strong uniaxial anisotropy of the Mn_4 unit, the field-induced transition is expected to be of first order like the spin-flip transition in a metamagnetic material and related to the flipping of the moment carried by the $\{Mn[N(CN)_2]_6\}^{4-}$ units. The temperature dependence of χ' versus H plots allows the monitoring of the spin-flip transition up to about 4.1 K and confirms the critical temperature previously determined by ac susceptibility and the field dependence of the magnetization. In a simple mean-field model that treats Mn_4 units as classical Ising spins and $\{Mn[N(CN)_2]_6\}^{4-}$ units as Heisenberg spins, it is possible to estimate J_{3D}/k_B at −0.030 K from the value of the critical field ($H_C=23$ kOe, $J_{3D}/k_B=-g\,\mu_B H_c/(2\,z\,k_B S_{Mn_4})$,[13a] in which z is the number of neighbors, that is, $z=z_{Mn_4}=z_{Mn}=6$ in this system). A rough estimation of J_{3D} can also be done based on the critical temperature (4.1 K): $J_{3D}/k_B=-3\,T_c/(2\,z\sqrt{S_{Mn_4}(S_{Mn_4}+1)\,S_{Mn}(S_{Mn}+1)})$.[15] The J_{3D}/k_B is found to be −0.037 K, which is in excellent agreement with the above estimation from the critical field H_c and published values.[10]

In summary, we have reported a unique 3D ferrimagnet ($T_C=4.1$ K) composed of the SMM Mn_4 building blocks ($S=9$) and paramagnetic Mn^{II} bridges ($S=5/2$). The strong uniaxial anisotropy of the Mn_4 unit and its magnetic coupling through magnetic linkage induces a spin-flip transition at 23 kOe and leads at higher fields to the parallel alignment of the two magnetic sublattices. To the best of our knowledge, this material is the first example in which an SMM complex has been used to design 3D ordered magnets. The enhancement of the magnetic inter-SMM interaction combined with the intrinsic properties of the SMM building block could open new perspectives in the design of high temperature anisotropic magnets.

Experimental Section

$\{Mn_4(hmp)_4(OH)_2Mn(dcn)_6\}\cdot 2MeCN\cdot 2THF$ (**1**): Hydroxymethylpyridine (218 mg, 2 mmol) and NEt_4OH with 20% water (736 mg, 1 mmol) was added to an acetonitrile solution (20 mL) containing $Mn(ClO_4)_2\cdot 6H_2O$ (362 mg, 1 mmol). The mixture was gently stirred at room temperature for one hour, then solid $NaN(CN)_2$ (89 mg, 1 mmol) was added. After the mixture had been stirred for a further hour, it was filtered, and the filtrate was carefully diffused in THF (40 mL) in a narrow glass tube ($\phi=6$ mm) to form brown block crystals of **1** (Yield: 31% based on Mn). Elemental analysis calcd for $C_{48}H_{48}N_{24}O_8Mn_5$: C 42.27, H 3.55, N 24.65; found: C 42.13, H 3.47, N 24.95. IR (KBr): $\tilde{\nu}=2299$ (s), 2241 (s), 2167 (s), 1606 (s), 1569 (m), 1481 (s), 1440 (s), 1359 (s), 1286 (m), 1253 (w), 1224 (w), 1157 (m), 1070 (s), 1047 (s), 914 (w), 889 (w), 823 (w), 765 cm^{-1} (s).

X-ray crystallographic analysis of **1**: Data collections were made on a Rigaku CCD diffractometer (Saturn70) with a graphite monochromated $Mo_{K\alpha}$ radiation ($\lambda=0.71069$ Å). The structures were solved by a direct method (SIR92)[16] and expanded by using Fourier techniques.[17] The non-hydrogen atoms were refined anisotropically, while hydrogen atoms were introduced as fixed contributors. Full-matrix least-squares refinements on F^2 based on 9108 unique reflections were employed, where the unweighted and weighted agreement factors of $R=\Sigma\,||F_o|-|F_c||/\Sigma\,|F_o|$ and $wR=[\Sigma w(F_o^2-F_c^2)^2/\Sigma w(F_o^2)^2]^{1/2}$ ($I>3.00\sigma(I)$) were used. A Sheldrick weighting Scheme was used. Plots of $\Sigma w(F_o^2-F_c^2)^2$ versus F_o^2, reflection order in data collection, $\sin\theta/\lambda$ and various classes of indices showed no unusual trends. Neutral atom scattering factors were taken from Cromer and Waber.[18] Anomalous dispersion effects were included in F_{calcd}; the values $\Delta f'$ and $\Delta f''$ were those of Creagh and McAuley.[19] The values for the mass attenuation coefficients are those of Creagh and Hubbel.[20] All calculations were performed by using the CrystalStructure crystallographic program.[21] Crystal data of **1**: $C_{48}H_{48}N_{24}O_8Mn_5$, $M_r=1363.75$, monoclinic $P2_1/n$ (no. 14), $T=160\pm 1$ K, $\lambda=0.71069$ Å, $a=14.386(5)$, $b=11.232(4)$, $c=19.251(7)$ Å, $\beta=103.704(5)°$, $V=3022.2(18)$ Å^3, $Z=2$, $\rho_{calcd}=1.499$ g cm^{-3}, $F_{000}=1386.00$. Final $R=0.066$, $wR=0.146$, GOF = 1.250 for 415 parameters and a total of 9108 reflections, 4292 unique ($R_{int}=0.035$) with $I>3.00\sigma(I)$; equivalent reflections were merged. The linear absorption coefficient, μ, for $Mo_{K\alpha}$ radiation is 1.086 mm^{-1}. An empirical absorption correction was applied which resulted in transmission factors ranging from 0.702 to 0.805. The data were corrected for Lorentz and polarization effects. Maximum positive and negative peaks in ΔF map were found to be $\rho_{max}=0.71$ e Å^{-3} and $\rho_{min}=-0.56$ e Å^{-3}.

CCDC-221351 contains the supplementary crystallographic data for this paper. These data can be obtained free of charge via www.ccdc.cam.ac.uk/conts/retrieving.html (or from the Cambridge

Crystallographic Data Centre, 12 Union Road, Cambridge CB2 1EZ, UK; fax: (+44) 1223-336-033; or deposit@ccdc.cam.ac.uk).

Received: October 15, 2003 [Z53093]

Keywords: cluster compounds · coordination modes · coordination polymers · magnetic properties · manganese

[1] a) J. Larionova, O. Kahn, S. Golhen, L. Ouahab, R. Clérac, *J. Am. Chem. Soc.* **1999**, *121*, 3349 – 3356; b) M. Ohba, N. Usuki, N. Fukita, H. Okawa, *Angew. Chem.* **1999**, *111*, 1911 – 1914 ; *Angew. Chem. Int. Ed.* **1999**, *38*, 1795 – 1798; c) J. S. Miller, *Adv. Mater.* **2002**, *14*, 1105 – 1110; d) J. R. Galán-Mascarós, K. R. Dunbar, *Angew. Chem.* **2003**, *115*, 2391 – 2395 ; *Angew. Chem. Int. Ed.* **2003**, *42*, 2289 – 2293; e) H. Miyasaka, H. Ieda, N. Matsumoto, K. Sugiura, M. Yamashita, *Inorg. Chem.* **2003**, *42*, 3509 – 3515.

[2] E. Coronado, J. R. Galán-Mascarós, C. J. Gómez-Garcia, V. Laukhin, *Nature* **2000**, *408*, 447 – 449.

[3] O. Sato, T. Iyoda, A. Fujishima, K. Hashimoto, *Science* **1996**, *272*, 704 – 705.

[4] Magnetism: A Supramolecular Function: Ed.: O. Kahn, *Nato ASI Ser. C* **1996**.

[5] Review: D. Gatteshi, R. Sessoli, *Angew. Chem.* **2003**, *115*, 278 – 309; *Angew. Chem. Int. Ed.* **2003**, *42*, 268 – 297, and references therein.

[6] W. Wernsdorfer, N. Aliaga-Alcalde, D. N. Hendrickson, G. Christou, *Nature* **2002**, *416*, 406 – 409.

[7] a) E. K. Brechin, J. Yoo, M. Nakano, J. C. Huffman, D. N. Hendrickson, G. Christou, *Chem. Commun.* **1999**, 783 – 784; b) J. Yoo, E. K. Brechin, A. Yamaguchi, M. Nakano, J. C. Huffman, A. L. Maniero, L.-C. Brunel, K. Awaga, H. Ishimoto, G. Christou, and D. N. Hendrickson, *Inorg. Chem.* **2000**, *39*, 3615 – 3623.

[8] I. D. Brown, D. Altermatt, *Acta Crystallogr. Sect. B* **1985**, *41*, 244 – 247.

[9] The polycrystalline samples for all magnetic measurements were restrained in nujol to avoid the partial reorientation of the crystals during magnetic measurements.

[10] The Curie constant is in good agreement with the value of 19.1 $cm^3 K mol^{-1}$ expected for three $S = 5/2$ Mn^{II} and two $S = 2$ Mn^{III} ions (with $g = 2$).

[11] a) S. R. Batten, P. Jensen, B. Moubaraki, K. S. Murray, R. Robson, *Chem. Commun.* **1998**, 439 – 440; b) M. Kurmoo, C. J. Kepert, *New J. Chem.* **1998**, *22*, 1515 – 1524; c) J. L. Manson, C. R. Kmety, Q. Z. Hunang, J. W. Lynn, G. M. Bendele, S. Pagola, P. W. Stephens, L. M. Liablesands, A. L. Rheingold, A. J. Epstein, J. S. Miller, *Chem. Mater.* **1998**, *10*, 2552 – 2560; d) J. L. Manson, C. D. Incarvito, A. L. Rheingold, J. S. Miller, *J. Chem. Soc. Dalton Trans.* **1998**, 3705 – 3706; e) P. Jensen, S. R. Batten, G. D. Fallon, B. Moubaraki, K. S. Murray, D. J. Price, *Chem. Commun.* **1999**, 177 – 178; f) J. L. Manson, C. R. Kmety, A. J. Epstein, J. S. Miller, *Inorg. Chem.* **1999**, *38*, 2552 – 2553; g) J. L. Manson, A. M. Arif, C. D. Incarvito, L. M. Liable-Sands, A. L. Rheingold, J. S. Miller, *J. Solid State Chem.* **1999**, *145*, 369 – 378; h) S. R. Marshall, C. D. Incarvito, J. L. Manson, A. L. Rheingold, J. S. Miller, *Inorg. Chem.* **2000**, *39*, 1969 – 1973; i) A. Escuer, F. A. Mautner, N. Sanz, R. Vicente, *Inorg. Chem.* **2000**, *39*, 1668 – 1673; j) I. Dasna, S. Golhen, L. Ouahab, O. Peña, J. Guillevic, M. Fettouhi, *J. Chem. Soc. Dalton Trans.* **2000**, 129 – 132; k) H. Miyasaka, R. Clérac, C. S. Campos-Fernández, K. R. Dunbar, *Inorg. Chem.* **2001**, *40*, 1663 – 1671.

[12] K. Kambe, *J. Phys. Soc. Jpn.* **1950**, *5*, 48.

[13] a) S. Chikazumi, *Physics of Ferromagnetism*, Clarendon Press, Oxford Science Publications, Oxford, **1997**, p. 521; b) A. Herpin, *Théorie du Magnétisme*, Blibliothèque des Sciences et Techniques Nucléaires, Presses Universitaires de France, Paris, **1968**, p. 620.

[14] a) M. Matsuura, Y. Okuda, M. Morotomi, H. Mollymoto, M. Date, *J. Phys. Soc. Jpn.* **1979**, *46*, 1031 – 1032; b) A. E. Clark, A. Callen, *J. Appl. Phys.* **1968**, *39*, 5972 – 5982.

[15] S. Ohkoshi, T. Iyoda, *Phys. Rev. B* **1997**, *56*, 11642 – 11652.

[16] SIR92: A. Altomare, M. C. Burla, M. Camalli, M. Cascarano, C. Giacovazzo, A. Guagliardi, G. Polidori, *J. Appl. Crystallogr.* **1994**, *27*, 435.

[17] DIRDIF99: P. T. Beurskens, G. Admiraal, G. Beurskens, W. P. Bosman, R. de Gelder, R. Israel, J. M. M. Smits, The DIRDIF99 program system, Technical Report of the Crystallography Laboratory, University of Nijmengen, The Netherlands, **1999**.

[18] D. T. Cromer, J. T. Waber, *International Tables for Crystallography* Vol IV, The Kynoch Press, Birmingham, England, **1974**, Table 2.2A.

[19] D. C. Creagh, W. J. McAuley, *International Tables for Crystallography*, *Vol. C* (Ed.: A. J. C. Wilson), Kluwer Academic Publishers, Boston, **1992**, pp. 219 – 222, Table 4.2.6.8.

[20] D. C. Creagh, J. H. Hubbell, *International Tables for Crystallography*, *Vol. C* (Ed.: A. J. C. Wilson), Kluwer Academic Publishers, Boston, **1992**, pp. 200 – 206, Table 4.2.4.3.

[21] CrystalStructure 3.15: Crystal structure analysis program, Rigaku and Rigaku/MSC, 9009 New Trails Dr. The Woodlands TX 77381, USA, **2000–2002**.

